

Antenna Pointing Error Estimation Using Conical Scan Technique and Kalman Filter

André L. G. Souza, Geovany A. Borges, João
Y. Ishihara, Henrique C. Ferreira, Renato A.

Borges
Department of Electrical Engineering
University of Brasilia
Brasilia, Brazil

andregama@lara.unb.br,
gaborges@ene.unb.br,

ishihara@ene.unb.br, hcferreira@unb.br,
raborges@ene.unb.br

Anatoly M. Kulabukhov, Vladimir A. Larin,
Vladimir V. Belikov

Department of Automatic Control Systems
Dnepropetrovsk National University
Dnepropetrovsk, Ukraine

vvbelikov@

Abstract—The present work proposes a different approach for the conical scan, a technique used to track the spacecraft position during the communication. The conical scan causes a variation of the received signal power and uses it to estimate the spacecraft position. The proposed technique applies the Kalman filter as the estimator and presented better results than the traditional one in non ideal scenarios. The proposal is evaluated by computer simulations and compared to others tracking techniques.

I. INTRODUCTION

Most of the spacecrafts must communicate with a ground station. The communication at the Ka-band have gained attention due to its availability and larger bandwidth when compared to C, X, and Ku-bands [1], [2]. The Ka-band is used in a variety of missions, for example deep space missions [3], [4], low earth orbit (LEO) satellites [5], and geostationary orbit satellites [6]. The main problem of employing high frequency systems is the antenna narrow beam width [7], which requires a better pointing accuracy. The spacecraft trajectory is usually predictable, so the antenna pointing reference can be set previously [8]. Unfortunately, there are cases in which the predicted trajectory differs from the real trajectory [9]. Also, disturbances like temperature gradient, wind forces, gravity forces, and manufacturing imperfections affect the beam pointing [10], [11]. All these effects make the beam position different than the pointing measured by the encoders, so they need to be compensated [11]. The spacecraft position relative to the beam can be estimated using radio frequency (RF) sensing techniques as feedback, for example monopulse and scanning techniques [12].

Monopulse techniques offer excellent results, but they are more complex than scanning techniques [13], requiring a specific hardware, carefully designed and manufactured, as described in [14], [15]. Scanning techniques are simpler and cheaper to implement, adding a movement to the original antenna path. The addition of small harmonic movements varies the received signal power. This approach is restricted

to carriers that do not contain amplitude modulation [9]. The analysis of the variation allows for to estimate the spacecraft position relative to the beam. Among three scanning techniques, conical, Lissajous, and rosette, the conical is a good choice due to the simplicity to implement without loss of performance [8]. The conical scan (conscan) is used in radar systems [16], missile tracking [17], spacecraft applications in deep space [13], [18], and spacecrafts in LEO [19]. Concerning the spacecraft applications, different methods were employed to solve the conscan problem. The work [20] applies least mean squares (LMS) batch estimator to solve it, and it is the most used approach for the problem. The report [21] tests the usage of the Kalman filter (KF) to estimate the spacecraft position, so the estimation can be performed in each sampling instant. Considering different sources of uncertainty, nonlinear techniques results are studied in [22].

The present work proposes a different solution for the conscan in spacecraft applications, applying the Kalman filter (KF) with three main differences than the proposal in [21]. The measurement function is mathematically manipulated instead of linearized by the Taylor series, one of the state variables is related to the carrier power, and the state vector is extended by its first-order time derivative. This modifications make the filter more robust to spacecraft movements and carrier power variations. In this way, some assumption made by the other techniques become unnecessary. The proposal increases the computational cost of the technique, but it is not a limitation, since the algorithm runs on the ground station computer. For now, the work is evaluated just in simulations, but it will be tested in the antenna to be built, at the University of Brasilia, in Brazil.

The work is divided as follows. Section II presents the traditional conscan technique, using the LMS technique. In Section III, the proposed approach is presented, modeling the problem in a different way and applying the KF to estimate the spacecraft position. The simulation results are presented in Section IV. Finally, the conclusions are discussed in Section V.

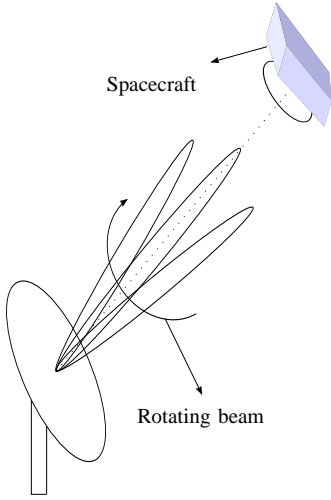


Fig. 1. Representation of the scan movement.

II. CONICAL SCAN

The traditional conscan technique will be explained in this section, and all the theory presented about it is based on [8], otherwise it will be explicitly cited. The conscan consists in the addition of harmonic movements in both axes, azimuth and elevation, making the antenna to perform a circular pattern while follows the spacecraft, as represented in Fig. 1. The antenna scan movement is circular with radius r and angular velocity ω . The radius of the scan must be small, so it does not significantly interfere with the communication. A good choice of the radius depends on the antenna characteristics, usually selected to decrease the maximum signal power up to 0.1 dB. The definition of the scanning angular velocity depends on the hardware capability, and the scan period is usually between 30 and 120 seconds. The antenna sample rate period T_s depends on the capability of the antenna RF hardware.

In Fig. 2, the frame of reference is presented. The origin represents the original antenna path, \mathbf{s}_k the spacecraft position, $\hat{\mathbf{s}}_k$ the estimated spacecraft position, \mathbf{a}_k the antenna position during the scan, and \mathbf{e}_k is the difference vector between the spacecraft and the antenna positions. The sub index k refers to the k -th sample performed at the time $t_k = kT_s$.

In the frame of reference, the antenna position is given by

$$\mathbf{a}_k = \begin{bmatrix} r \cos \omega t_k \\ r \sin \omega t_k \end{bmatrix}, \quad (1)$$

and

$$\mathbf{e}_k = \mathbf{s}_k - \mathbf{a}_k = \begin{bmatrix} e_{a,k} \\ e_{e,k} \end{bmatrix} = \begin{bmatrix} s_{a,k} - r \cos \omega t_k \\ s_{e,k} - r \sin \omega t_k \end{bmatrix} \quad (2)$$

The sub indexes e and a refer to elevation and azimuth axes, respectively.

The received power p_k can be approximated by

$$p_k = p_{0,k} \exp\left(-\mu \frac{\epsilon_k^2}{h^2}\right) + v_k, \quad (3)$$

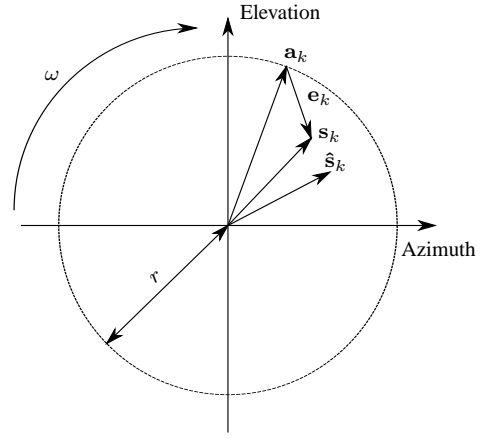


Fig. 2. Pointing reference system.

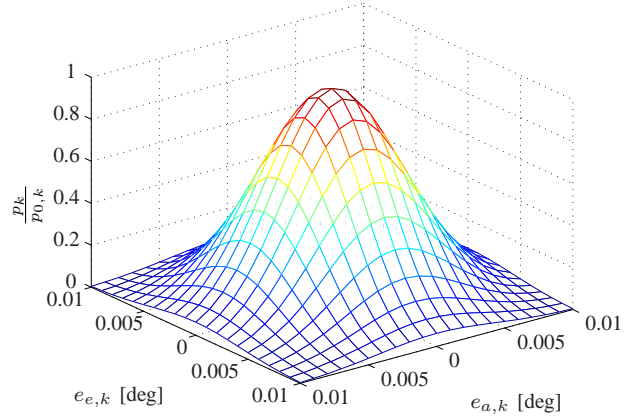


Fig. 3. Relation between the carrier power and the pointing error.

where $p_{0,k}$ is the carrier power, $\mu = 4 \ln 2$ is a constant, h is the antenna beam width, v_k is an additive Gaussian white noise, and ϵ_k^2 is the squared total error, given by

$$\epsilon_k^2 = \mathbf{e}_k^T \mathbf{e}_k = \mathbf{s}_k^T \mathbf{s}_k - 2\mathbf{a}_k^T \mathbf{s}_k + r^2. \quad (4)$$

Fig. 3 shows the relation between the received power and the axes pointing error. Due to the harmonic movements, the received power varies in a sinusoidal shape during the scan, with the amplitude depending on the spacecraft position.

During a scan period, the traditional technique considers the spacecraft position constant, from now on denoted by \mathbf{s} . This assumption is acceptable if the measurements are sampled in small intervals of time and the distance between the spacecraft and the ground station is long enough, making the spacecraft position varies slowly. The carrier power is considered constant as well, so it will be denoted by p_0 .

The first-order Taylor expansion is applied to make (3) linear, becoming

$$p_k = p_0 \left[1 - \mu \frac{\epsilon_k^2}{h^2} \right] + v_k. \quad (5)$$

Replacing (4) in (5), it becomes

$$p_k = p_m + \frac{2p_0 \mu r}{h^2} (s_a \cos \omega t_k + s_e \sin \omega t_k) + v_k, \quad (6)$$

where p_m is the mean received power during the scan, given by

$$p_m = p_0 \left[1 - \frac{\mu}{h^2} (r^2 + \mathbf{s}^T \mathbf{s}) \right], \quad (7)$$

and it is computed using the mean of the received measurements during a scan period. The difference between the received power and the mean power is given by

$$dp_k = p_k - p_m = g s_a \cos \omega t_k + g s_e \sin \omega t_k + v_k, \quad (8)$$

where

$$g = \frac{2p_0 \mu r}{h^2}. \quad (9)$$

Making $m_k = g [\cos \omega t_k \quad \sin \omega t_k]$, (8) can be rewritten as

$$dp_k = m_k \mathbf{s} + v_k. \quad (10)$$

Gathering measurements during a scan period, the spacecraft position can be estimated using LMS, and it is given by

$$\hat{\mathbf{s}} = \left[(\mathbf{M}^T \mathbf{M})^{-1} \mathbf{M}^T \right] \mathbf{d}\mathbf{p}, \quad (11)$$

where \mathbf{M} and $\mathbf{d}\mathbf{p}$ are vectors, with stored values of m_k and dp_k , respectively.

Although it is a very used technique, the conscan has some drawbacks. Depending on the sampling rate and on the scan period, the spacecraft position and carrier power sometimes can not be considered constants during the scan period, and the conscan with the LMS estimator can not be used. The necessity of waiting for a full scan cycle can become a restriction, as described in [24] for example.

III. PROPOSED TECHNIQUE

The proposed technique employs the KF to estimate s_k . The theory about the discrete KF can be found in many textbooks, for example [23]. The author of [21] proposed a conscan technique based on the KF, but in a different way. In [21], the state vector is the spacecraft position, considered constant and disturbed by a Gaussian white noise in each sampling instant. The measurement equation is (8), and the author considers the carrier power constant during the scan period. The present work does not approximate (3) by the Taylor series, instead of that, a mathematical manipulation is performed, avoiding linearization errors. The proposition tracks not only the spacecraft position, but also a variable related to the carrier power. Also, the state vector is extended by its first-order time derivatives, becoming more robust to variations of the state vector dynamics.

Disregarding v_k and considering (3) a deterministic function, the logarithmic function can be applied to it, so it becomes

$$\ln p_k = \ln p_{0,k} - \mu \frac{\epsilon_k^2}{h^2}. \quad (12)$$

All the uncertainty about the model must be assigned to the Gaussian white noise w_k with zero mean and covariance W . Replacing (4) in (12), and considering the model uncertainty, (12) becomes

$$\ln p_k = \Delta_k + \frac{2\mu r}{h^2} (s_{a,k} \cos \omega t_k + s_{e,k} \sin \omega t_k) + w_k, \quad (13)$$

where

$$\Delta_k = \ln p_{0,k} - \frac{\mu}{h^2} (s_{a,k}^2 + s_{e,k}^2 + r^2). \quad (14)$$

The variance of w_k can be taken experimentally, defined as

$$W = \sigma_p^2. \quad (15)$$

The state vector \mathbf{x}_k is composed of Δ_k , $s_{a,k}$, and $s_{e,k}$, and it is extended by the first-order time derivatives of the state variables, represented by $\dot{\Delta}_k$, $\dot{s}_{a,k}$, and $\dot{s}_{e,k}$, respectively. The state vector is

$$\mathbf{x}_k = \left[\Delta_k \quad \dot{\Delta}_k \quad s_{a,k} \quad \dot{s}_{a,k} \quad s_{e,k} \quad \dot{s}_{e,k} \right]^T. \quad (16)$$

The evolution function is modeled as

$$\mathbf{x}_k = \begin{bmatrix} 1 & T_s & 0 & 0 & 0 & 0 \\ 0 & 1 & 0 & 0 & 0 & 0 \\ 0 & 0 & 1 & T_s & 0 & 0 \\ 0 & 0 & 0 & 1 & 0 & 0 \\ 0 & 0 & 0 & 0 & 1 & T_s \\ 0 & 0 & 0 & 0 & 0 & 1 \end{bmatrix} \mathbf{x}_{k-1} + \mathbf{q}_{k-1}. \quad (17)$$

In this equation, \mathbf{q}_{k-1} is a Gaussian white noise vector, with covariance matrix \mathbf{Q} . The time derivative variables are modeled as constants disturbed by random noise.

The standard deviation of the spacecraft position depends on the application, modeled as the maximum drift in one period, and the standard deviation of Δ depends on the sensor standard deviation σ_p . The variances of the state variables time derivatives are modeled 100 times smaller than the respective variables variances.

The covariance matrix

$$\mathbf{Q} = \text{diag} (\sigma_\Delta^2, 10^{-2}\sigma_\Delta^2, 10^{-2}, 10^{-4}, 10^{-2}, 10^{-4}) \quad (18)$$

was set empirically for the simulation, where

$$\sigma_\Delta = \sigma_p. \quad (19)$$

The measurement function is linear concerning the state variables, and it can be written as

$$\ln p_k = \mathbf{C}_k \mathbf{x}_k + \mathbf{w}_k, \quad (20)$$

where

$$\mathbf{C}_k = \left[1 \quad 0 \quad \frac{2\mu r}{h^2} \cos \omega t_k \quad 0 \quad \frac{2\mu r}{h^2} \sin \omega t_k \quad 0 \right]. \quad (21)$$

Using the proposed formulation, the state vector can be estimated in every sampling period using the KF.

The filter directly estimates the spacecraft position, but not the carrier power. Using (14), the carrier power can be computed using the estimated state. Employing this technique, it is possible to estimate the spacecraft position and the carrier power, even if the measurement is not available.

The initial state vector assumes the same initial carrier power as the traditional technique, so it is

$$\hat{\mathbf{x}}_0 = \left[\left(\ln p_0 - \frac{\mu r^2}{h^2} \right) \quad 0 \quad 0 \quad 0 \quad 0 \quad 0 \right]^T. \quad (22)$$

The initial covariance matrix $\hat{\mathbf{P}}_0$ does not have a deterministic way to be defined, but it must denote a great level of uncertainty, considering reasonable values for the variables. In this case, it was defined as

$$\hat{\mathbf{P}}_0 = \text{diag}(10 \ln p_0, 10 \ln p_0, 1, 1, 1, 1). \quad (23)$$

IV. SIMULATIONS AND RESULTS

Simulations were performed in order to evaluate the proposed technique. As a normal assumption in the literature about scanning techniques, it is considered that the antenna can perfectly follow the reference position. The proposed technique is tested for different cases, similar to the ones presented in [8], [21]. A summary of the tests is presented in Table I. Despite being theoretical tests, they help to visualize the performance in situations different than the perfect one, for example when the spacecraft suddenly varies its position (Test B), when the spacecraft real position varies faster than the predicted (Test C), and when there is a wrong assumption about the carrier power (Test F).

TABLE I
SIMULATION CASES.

Test ID	$\ s_k\ $	$p_{0,k}$
A	Constant	Constant
B	Step	Constant
C	Ramp	Constant
D	Constant	Ramp
E	Ramp	Ramp
F	Constant	Constant and different than the real one

The tests parameters are $\omega = \pi/16$ rad/s, $p_0 = 4.14 \cdot 10^{-13}$ W, $T_s = 1$ s, $r = 5.9$ mdeg, $h = 65$ mdeg, and $\sigma_p = 1.9356$, except for p_0 when it drifts. The results for tests root mean squared (RMS) error can be seen in Table II, where **TT** refers to the traditional technique described in Section II, **KF1** to the algorithm proposed in [21], and **KF2** to the algorithm proposed here.

The proposed technique has smaller RMS error than the others techniques, except in Test A, the most unlikely to happen since it is an ideal situation. The proposed technique result for the Test A is worse than the others due to the model, which considers the state vector time derivatives. Any

TABLE II
RMS ERROR RESULTS FOR \hat{s}_k IN THE TESTS WITH ALL MEASUREMENTS.

Test	TT [mdeg]	KF1 [mdeg]	KF2 [mdeg]
A	6.48	17.54	18.39
B	10.11	12.04	5.31
C	7.52	7.06	1.60
D	17.38	9.47	3.02
E	23.31	1.58	0.98
F	9.54	20.69	4.57

variation in these variables increases the estimation RMS error because the spacecraft position is constant during the simulation. The technique has a characteristic of handling with the spacecraft position variation and wrong assumption of the carrier power. For the Tests B, C, D, E, and F, when compared to the traditional technique, the RMS error is reduced in approximately 47%, 78%, 82%, 95%, and 52%, respectively. As visual example, the results for the Tests B, C, E, and F can be seen in Fig. 4, Fig. 5, Fig. 6, and Fig. 7. All the results showed the proposed technique robustness against changes in the beam pointing, and adaptability when compared to the others.

The task of tracking the carrier power was also accomplished, even when it drifts (Test , as presented in Fig. 8.

V. CONCLUSIONS

A different approach for the conscan method was proposed in order to improve the technique. The nonlinear equation relating the spacecraft position and the received power is not linearized by the Taylor series. Instead, a mathematical manipulation is applied to the exponential function, making the measurement model linear with respect to the state variables, and avoiding linearization errors. Since the model is linear, the KF is used to track the spacecraft position considering dynamics that the eventual technique does not consider.

There are two main advantages of the proposed technique, performance and cost. The tests showed that the proposed technique had a better performance when compared to the others in most of the tested situations. The assumption of constant carrier power during the scan was avoided, and, more than that, the carrier power was estimated. The assumption of constant spacecraft position, which was a limitation for some missions, was also avoided, and the spacecraft position could be estimated in each sampling instant. The proposed technique may replace the monopulse based techniques in some missions, since the monopulse is a more expensive and complex technique category.

The characteristic of handling with the spacecraft position and carrier power variations decreases the performance in the ideal scenario, but such a scenario is unlikely to occur, but maybe it can be solved using different adjustments of the covariance matrix, which were not tested so far. The technique increases the computational cost because there are matrix calculations in each sampling instant, but since the

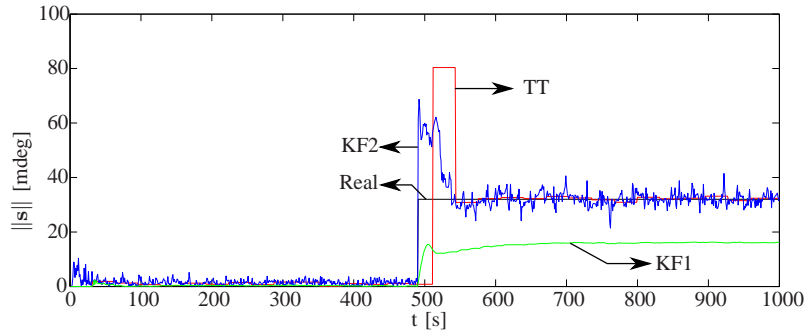


Fig. 4. Results of Test B.

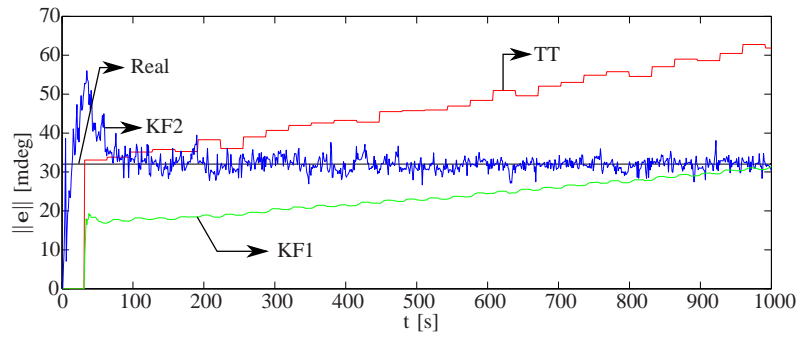


Fig. 5. Results of Test D.

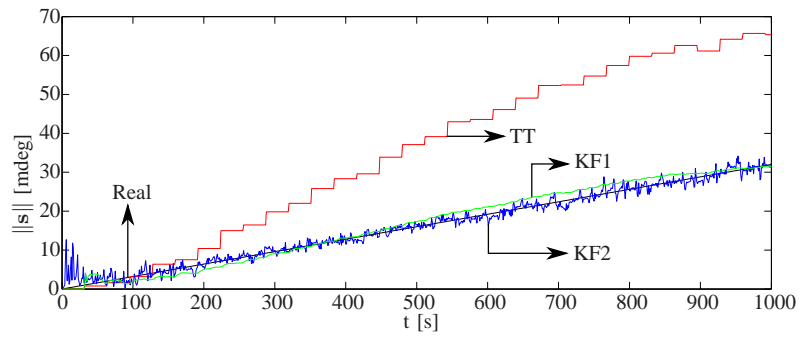


Fig. 6. Results of Test E.

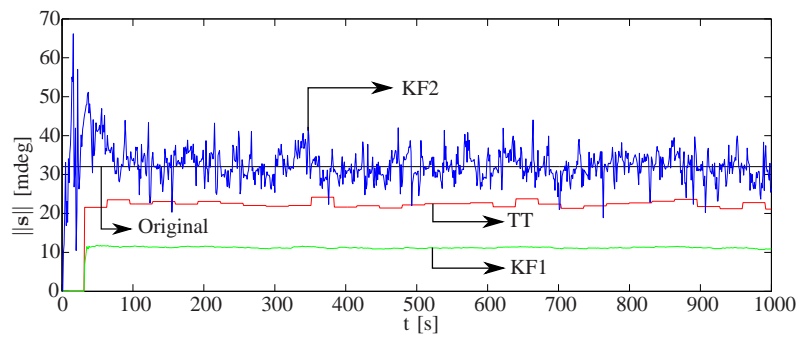


Fig. 7. Results of Test F.

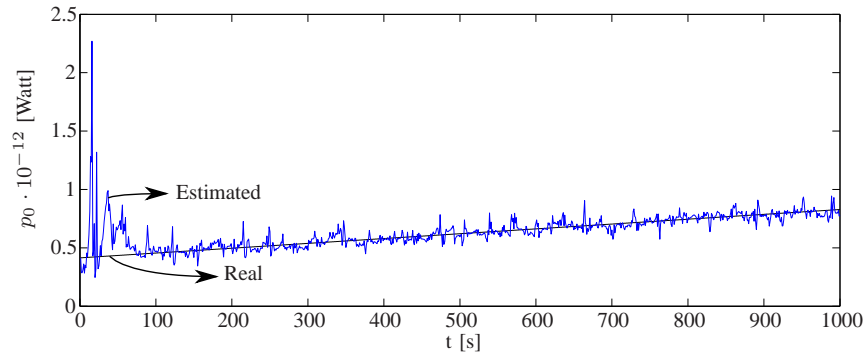


Fig. 8. Results of p_0 tracking in Test E.

algorithm runs on a ground station computer, it is not a limitation.

As future works, it is important to evaluate the technique in practical tests, since it was only simulated so far. Some tests are intended to be performed in the satellite ground station that will soon be built at the University of Brasilia, Brazil. Since the proposed technique can be used instead of the monopulse based techniques, a comparison must be made between them. It is proposed, also as future work, to evaluate the usage of the estimator presented here as part of the feedback in the antenna control system, allowing to reduce the costs of the encoders.

ACKNOWLEDGMENT

Part of the work was developed as an internship at the National University of Dnepropetrovsk (DNU), in Ukraine. The internship was sponsored by the Brazilian National Council for Scientific and Technological Development (CNPq) and the Brazilian Space Agency (AEB).

REFERENCES

- [1] J. Jena and P. K. Sahu, Rain fade and Ka-band Spot Beam Satellite communication in India, in *Recent Advances in Space Technology Services and Climate Change (RSTSCC)*, 304-306, 2010.
- [2] T. V. Omotosho, J. S. Mandeep, and M. Abdullah, Atmospheric gas impact on fixed satellite communication link a study of its effects at Ku, Ka and V bands in Nigeria, in *2011 IEEE International Conference on Space Science and Communication*, 69-72, 2011.
- [3] A. N. Curren, J. A. Dayton Jr, R. W. Palmer, K. J. Long, D. A. Force, C. E. Weeder, Z. A. Zachar, and W. L. Harvey, The Cassini mission Ka-band TWT, in *International Electron Devices Meeting*, 783-786, 1994.
- [4] S. Shambayati, The Struggle for Ka-band: NASA's Gradual Move Towards Using 32-GHz Ka-band for Deep Space Missions, in *Aerospace Conference*, 1-21, 2007.
- [5] W. Li, C. L. Law, and V. Dubey, A novel ARQ-based multistep power control scheme for Ka-band LEO satellite CDMA systems, in *IEEE International Conference on Communications*, Vol.9, 2625-2629, 2001.
- [6] M. Hein, H. Bayer, A. Kraus, R. Stephan, C. Volmer, A. Heuberger, E. Eberlein, C. Keip, M. Mehnert, A. Mitschele-Thiel, P. Dries, and T. Volkert, Perspectives for mobile satellite communications in Ka-band (MoSaKa), in *Proceedings of the Fourth European Conference on Antennas and Propagation*, 1-5, 2010.
- [7] B. R. Elbert, *The Satellite Communication Ground Segment and Earth Station Handbook*, Norwood: Artech House, Chap. 2, 2001.
- [8] W. Gawronski, and E. Craparo, Antenna scanning techniques for estimation of spacecraft position, in *IEEE Aerospace Conference Proceedings*, Vol.2, 939-948, 2002.
- [9] G. J. Hawkins, D. J. Edwards, and J. P. McGeehan, Tracking systems for satellite communications, in *IEEE Proceedings of Communications, Radar and Signal Processing*, Vol.135, No.5, 393-407, 1988.
- [10] W. Gawronski, F. Baher, and O. Quintero, Azimuth-track level compensation to reduce blind-pointing errors of the Deep Space Network antennas, *IEEE Antennas and Propagation Magazine*, Vol.42, No.2, 28-38, 2000.
- [11] W. Gawronski, *Modeling and Control of Antennas and Telescopes*, New York: Springer, 2008.
- [12] R. Dang, B. Watson, I. Davis, and D. Edwards, Electronic Tracking Systems for Satellite Ground Stations, in *15th European Microwave Conference*, 681-687, 1985.
- [13] P. Besso, M. Bozzi, M. Gormaggi, and L. Perregrini, Pointing enhancement techniques for deep-space antennas, *International Journal of Microwave and Wireless Technologies*, Vol.2, No.2, 211218, 2010.
- [14] S. H. M. Armaki, F. H. Kashani, J. R. Mohasel, and M. Nasser-Moghadas, Design and Realization of Tracking Feed Antenna System, in *IEICE Electronics Express*, Vol.8, No.12, 908-915, 2011.
- [15] H. Bayer, A. Krauss, R. Stephan, and M. Hein, A dual-band multimode monopulse tracking antenna for land-mobile satellite communications in Ka-band, in *6th European Conference on Antennas and Propagation*, 2357-2361, 2012.
- [16] G. M. Brooker, Conical-scan antennas for W-band radar systems, *Proceedings of the International Radar Conference*, 406-411, 2003.
- [17] W. Schmitendorf, Y. Kao, and H. Hwang, Robust tracking controller for a seeker scan loop, *IEEE Transactions on Control Systems Technology*, Vol.7, No.2, 282-288, 1999.
- [18] J. E. Ohlson, and M. S. Reid, Conical-Scan Tracking With the 64-meter Antenna at Goldstone, Tech. Rep., Jet Propulsion Laboratory, 1976.
- [19] J. Nateghi, L. Mohammadi, and G. R. Solat, Analysis of the four-horn monopulse for LEO satellite tracking using the exact model, in *11th International Conference on Advanced Communication Technology*, Vol.2, 1349-1352, 2009.
- [20] L. S. Alvarez, Analysis of Open-Loop Conical Scan Pointing Error and Variance Estimators, Tech. Rep., Jet Propulsion Laboratory, 1993.
- [21] D. B. Eldred, An Improved Conscan Algorithm Based on a Kalman Filter, Tech. Rep., Jet Propulsion Laboratory, 1994.
- [22] L. Chen, N. Fathpour, and R. K. Mehra, Comparison Antenna Conical Scan Algorithms for Spacecraft Position Estimation, *Journal of Guidance, Control and Dynamics*, Vol.30, No.4, 1186-1189, 2007.
- [23] D. Simon, *Optimal State Estimation*. New Jersey: Wiley Interscience, Chap. 5, 2006.
- [24] J. B. Berner, A. M. Bhanji and S. C. Kurtik, Changes in the Deep Space Network to support the Mars Reconnaissance Orbiter, In *SpaceOps Earth, Moon, Mars, and Beyond*, AIAA, 1-7, 2006.